Reaction Rate Closure for Turbulent Detonation Propagation through CLEM-LES

Brian Maxwell , Matei Radulescu
Department of Mechanical Engineering, University of Ottawa
161 Louis Pasteur, Ottawa, K1N 6N5, Canada
Sam Falle
School of Applied Mathematics, University of Leeds
Leeds, LS2 9JT, UK
Gary Sharpe
Blue Dog Scientific Ltd.
1 Mariner Court, Wakefield, WF4 3FL, UK

1 Introduction

In the current work, turbulent and unstable detonation propagation is modelled using a novel combustion modelling strategy which treats highly compressible and reactive flows involving very rapid transients in pressure and energy. Previously, the detonation phenomena has been investigated by solving Euler's equations of fluids motion, which do not account for turbulent mixing or molecular diffusion. Although such attempts have provided limited insight into the roles that shock compression or turbulent motions may have on detonation propagation, the solutions obtained were subject to changes in resolution and did not converge to unique solutions [1]. Furthermore, this approach is problamatic since a highly unstable detonation front gives rise to unburned pockets of fuel in its wake. These pockets then burn out, relatively quickly, through molecular diffusion enhanced by turbulent mixing. More recent modelling attempts through Direct Numerical Simulation (DNS) of the Navier-Stokes (N-S) equations address this problem by resolving the full spectrum of scales present, but are limited to providing insight only on single-isolated events, such as triple point collisions [2]. In order to address these fundamental short comings associated with Euler simulations or DNS, a reasonable compromise between accuracy of solution and resolvability is to employ Large Eddy Simulation (LES). For LES, the large scale fluid motions, governed by the N-S equations, are solved directly using numerical methods. The unresolved, micro-scale turbulence, is then modelled as a supplement to the large scale numerical solutions. A recent study [3] demonstrates that LES can be used to provide insight on the sub-grid effects that contribute to the unstable detonation reaction rate. Closure to the reaction rate, however, remains difficult to resolve as it is typically obtained by assuming either instantaneous mixing or reaction at the subgrid scale.

The LES strategy adopted here is an extension of the compressible-LEM (CLEM) subgrid strategy [4] based on the Linear Eddy Model for Large Eddy Simulation (LEM-LES) [5], which does not rely on bold assumptions regarding the mixing or reaction rates. In the past, LEM-LES has been successfully applied to model weakly compressible turbulent flames [6, 7], and also supersonic inert mixing layers

Correspondence to: bmaxwell@uottawa.ca

[8]. Only recently has the CLEM subgrid approach been successful to treat highly compressible and reactive flows, which involve very rapid transients in pressure and energy. In various 1-D problems, the CLEM subgrid strategy has been shown to capture laminar and turbulent flame speeds as well as detonation propagation and initiation events [4]. In the CLEM-LES context, the subgrid is treated as a 1-D sample of a diffusion-reaction system within each LES cell. This is intended to reduces the expense of solving a complete multi-dimensional problem through DNS while preserving micro-scale hot spots and their physical effects on ignition. Thus, the model provides high resolution closure for the unresolved chemical reaction terms in the governing, LES-filtered, reactive N-S equations.

In this paper, the CLEM-LES approach is applied to simulate two-dimensional, unobstructed, detonation propagation in a narrow channel at low pressures. The parameters of the model are chosen to mimic the premixed methane-oxygen mixture of experiments conducted at the University of Ottawa [9]. Additional closure for the unresolved turbulent viscosity is provided by a one-equation Localized subgrid Kinetic energy Model (LKM). In this paper, CLEM-LES is demonstrated to reproduce the correct qualitative propagation characteristics, and a converged burning rate that is comparable to experimental observation.

2 Modelling Approach: Filtered LES Equations

For flows which are highly transient, turbulent, compressible, and involve rapid combustion chemistry, the gas dynamic evolution is governed by the compressible N-S equations. In order to address the difficulty of resolving the full spectrum of length scales resulting from the presence of large flow velocities with high Mach numbers (M_a) and Reynolds numbers (R_e), the unresolved scales of the governing equations are filtered and modelled through the LES approach. In this respect, rapid transients and fluid motions are captured on the large scales, while the small scale contributions are modelled through source terms. The LES-filtered conservation equations for mass, momentum, and energy of a calorically perfect fluid system are given below in Equations 1 through 3, respectively. The set of equations is further supplemented by a one-equation Localized Kinetic energy Model (LKM) to describe the evolution of subgrid velocity fluctuations in the form of subgrid kinetic energy k^{sgs}, see equation 4. Finally, the equations of state are given by 5. It should be noted that the equations are given in non-dimensional form where the various gas properties are normalized by the reference quiescent state. Favre-average filtering is achieved by letting $\tilde{f} = \overline{\rho f}/\bar{\rho}$, where f represents one of the many state variables. Here ρ, p, e, T, and $\boldsymbol{u}$ refer to density, pressure, internal energy, temperature, and velocity vector, respectively.

$$\frac{\partial \bar{\rho}}{\partial t} + \nabla \cdot (\bar{\rho}\tilde{\boldsymbol{u}}) = 0 \tag{1}$$

$$\frac{\partial \bar{\rho}\tilde{\boldsymbol{u}}}{\partial t} + \nabla \cdot (\bar{\rho}\tilde{\boldsymbol{u}}\tilde{\boldsymbol{u}}) + \nabla \bar{p} - \nabla \cdot \bar{\rho}(\nu + \nu_t)\left(\nabla \tilde{\boldsymbol{u}} + (\nabla \tilde{\boldsymbol{u}})^T - \frac{2}{3}(\nabla \cdot \tilde{\boldsymbol{u}})\hat{I}\right) = 0 \tag{2}$$

$$\frac{\partial \bar{\rho}\tilde{e}}{\partial t} + \nabla \cdot \left((\bar{\rho}\tilde{e} + \bar{p})\tilde{\boldsymbol{u}} - \tilde{\boldsymbol{u}} \cdot \bar{\tau}\right) - \left(\frac{\gamma}{\gamma - 1}\right)\nabla \cdot \left(\bar{\rho}(\frac{\nu}{P_r} + \frac{\nu_t}{P_{r,t}})\nabla \tilde{T}\right) = -Q\overline{\dot{\omega}} \tag{3}$$

$$\frac{\partial \bar{\rho}k^{sgs}}{\partial t} + \nabla \cdot (\bar{\rho}\tilde{\boldsymbol{u}}k^{sgs}) - \nabla \cdot \left(\frac{\bar{\rho}\nu_t}{P_{r,t}}\nabla k^{sgs}\right) = \bar{\rho}\nu_t\left(\nabla \tilde{\boldsymbol{u}} + (\nabla \tilde{\boldsymbol{u}})^T - \frac{2}{3}(\nabla \cdot \tilde{\boldsymbol{u}})\hat{I}\right) \cdot (\nabla \tilde{\boldsymbol{u}}) - \bar{\rho}\epsilon \tag{4}$$

$$\tilde{e} = \frac{\bar{p}/\bar{\rho}}{(\gamma - 1)} + \frac{1}{2}\tilde{\boldsymbol{u}}\tilde{\boldsymbol{u}} + \frac{1}{2}k^{sgs} \qquad \text{and} \qquad \bar{\rho}\tilde{T} = \bar{p} \tag{5}$$

Other usual properties to note are the heat release, Q, the ratio of specific heats, γ, and the kinematic viscosity, ν. The turbulent viscosity and dissipation are modeled according to $\nu_t = C_\nu\sqrt{k^{sgs}}h$ and $\epsilon = C_\epsilon(k^{sgs})^{3/2}/h$, respectively. Here, h is the minimum grid spacing. Also, it should be noted that C_ν and C_ϵ are model constants which require calibration. In this study, $C_v = 0.06$ and $C_\epsilon = 1.0$ were chosen. Finally, the chemical reaction term, $\overline{\dot{\omega}}$, requires closure.

3 1-D Subgrid model for the CLEM-LES Strategy

In order to implement the CLEM-LES strategy, the micro-scale mixing and chemical reaction is handled entirely on the subgrid. Here, the subgrid model applied is a 1-D representation of the flow field within each LES cell whose orientation is aligned in the direction of local flow. To derive the sub-grid model formulation, pressure gradients are locally neglected within the small scales of each LES cell. Thus, low-Mach number approximations are applied to treat the small scales while the pressure on the large scales is treated using piece-wise constant discretization of the flow field. Therefore, the pressure field evolution is solved entirely on the LES. The large scale pressure changes from the LES are then prescribed to the subgrid, as a source term, in order to account for energy changes due to rapid compression or expansions. This formulation was previously applied to determine ignition limits of idealized non-turbulent and rapidly expanding hydrogen jets [10]. However, in this new approach, the total energy release due to chemical reaction, $\overline{\dot{\omega}}$, is computed at each time step and accounted for in the LES, Equation 3. Therefore, the system of equations that is solved on the subgrid is the conservation of enthalpy, Equation 6, and the conservation of reactant mass, Equation 7. The source terms, $\dot{F_T}$ and $\dot{F_Y}$ account for the effect of turbulence on the subgrid in the form of random "stirring" events [11] and m is a one-dimensional mass weighted coordinate whose transformation to Cartesian spatial coordinates is given by Equation 8. Finally, the reaction term, $\dot{\omega}$, can be directly computed on the small scales at each subgrid node. In this case, a one-step Arrhenius combustion model is assumed through Equation 9.

$$\rho\frac{DT}{Dt} - \left(\frac{\gamma-1}{\gamma}\right)\frac{\partial p}{\partial t} - \rho\frac{\partial}{\partial m}\left(\rho^2\frac{\nu}{P_r}\frac{\partial T}{\partial m}\right) = -\left(\frac{\gamma-1}{\gamma}\right)Q\dot{\omega} + \dot{F_T} \tag{6}$$

$$\rho\frac{DY}{Dt} - \rho\frac{\partial}{\partial m}\left(\rho^2\frac{\nu}{L_e P_r}\frac{\partial Y}{\partial m}\right) = \dot{\omega} + \dot{F_Y} \tag{7}$$

$$m(x,t) = \int_{x_o}^{x}\rho(x,t)dx \tag{8}$$

$$\dot{\omega} = -\rho A Y e^{(-E_a/T)} \tag{9}$$

Here, only premixed combustion is considered with a single reactant species, with mass fraction Y. Finally, the subgrid model formulation differs from previous LEM-LES implementations [6–8] for two reasons. First, the pressure term in Equation 6 accounts for the energy changes associated with rapid changes in pressure. Second, the 1-D sub-grid domains are formulated with Lagrangian mass-weighted coordinates, m. This is done in order to account for the local expansion or contraction of the fluid along particle paths, and also changes in spatial distance between computational nodes on the subgrid (dx). Further details of the pressure coupling and LEM stirring procedure are found elsewhere [4].

4 Turbulent Detonation Wave Structure and Propagation Characteristics

In the current study, unobstructed detonation propagation is simulated in a 2-D channel, $900\lambda_{1/2}$ long by $20\lambda_{1/2}$ high, where $\lambda_{1/2}$ is the ZND half reaction length. The non-dimensional activation energy, heat release, and pre-exponential factor are $E_a = 34.26$, $Q = 50.30$, and $A = 718.27$ respectively. The viscosity was set to $\nu = 3.62\text{x}10^{-3}$ with $L_e = 1.33$ and $P_r = 0.723$. These parameters are tuned to match detonation and flame propagation behaviour for stoichiometric methane-oxygen mixtures at $\hat{p_o} = 3.5$kPa and $\hat{T_o} = 300$K. Specifically, these parameters reproduce a detonation with a velocity of $D_{CJ} = 6.30$ and a half-reaction length of $\lambda_{1/2} = 9.68$mm. The detonation wave is initiated by imposing an over-driven ZND structure $20\lambda_{1/2}$ from the left boundary. A wall-type boundary on the left acts to decelerate the wave from the over-driven state to CJ conditions after an initial transient. Finally, to initiate 2-D cellular instability in the wave, a region of random perturbations to the density field is

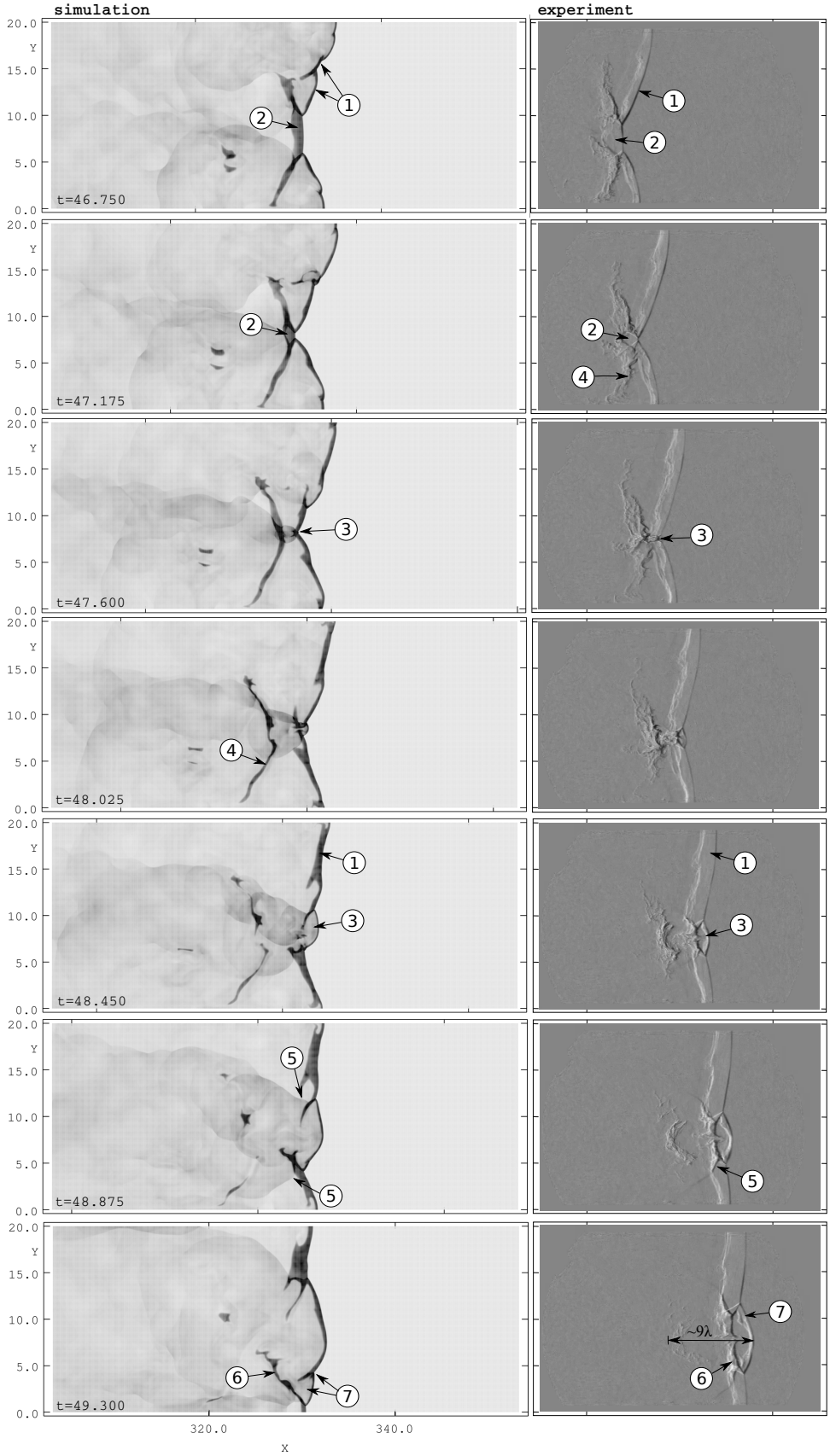

Figure 1: Numerical density evolution (left) and corresponding experimental Sclieren photography [9] (right) of a detonation triple point collision process.

introduced for a distance of $4\lambda_{1/2}$ ahead of the initial wave. The simulations are then run for sufficient time for the wave to decelerate to the CJ velocity.

A visual comparison of a flow field, obtained through resolved LES and the corresponding experiment [9], is shown in Figure 1 for an instance where a triple-point collision occurs for a detonation whose cell size is comparable to the channel height. For the LES, the density evolution is shown for various instances of the collision process. The base resolution of the simulation is $h = (\lambda_{1/2}/32)$ on the supergrid, with a further $N = 24$ subgrid nodes within each supergrid cell. For the experiment [9], Schlieren images of each corresponding instance are obtained from high speed photography and are also shown in the Figure. For comparison, many features are noted in the Figure (1-7). The first feature (1), is a Mach shock with a turbulent reaction zone that follows closely. In both the simulation, and the experiment, the reaction zone is slightly decoupled from the shock owing to local unsteadiness of the wave front. This can be seen by the thickening of the shocked unburned gas region as time evolves. In the LES, however, this wave appears to be more irregular, containing what appears to be a smaller and less pronounced cell structure (cells within cells). It should be noted that experimental observations [9] report a very stochastic nature of the propagating wave. In this sense, random bifurcations on wave fronts and changes in cell patterns are expected. Feature (2) is a completely decoupled incident shock-reaction zone, as can be seen by the large region of dense unburned gas. As the two triple-points approach each other, transverse shock waves compress this gas further. At the focal point of the collision, owing to the increased pressure and temperature, the unburned pocket (2) ignites very rapidly. This "explosion", noted by feature (3), drives transverse shock waves and a strong Mach shock forward coupled with very rapid burning. Feature (4) is a pocket of unburned gas which is not ignited by compression associated with the original Mach shocks (1). Instead, these pockets mix and burn along turbulent shear layers. Thus, Kelvin-Helmholtz instability gives rise to increased burning rates through turbulent mixing of the burned and unburned gases. Furthermore, Richtmyer-Meshkov instability further enhances combustion of of feature (4) via shock compression associated with the transverse shocks, labelled as feature (5), which originate from feature (3). Feature (6) is a new pocket of unburned gas that forms along slip lines associated with the collision process. Finally, feature (7) is a bifurcation observed on the Mach shock of feature (3), owing to the unstable nature of methane-air detonations. This bifurcation also occurs in the experiment but is less pronounced. Although features (1-7) are captured by the LES, a key difference is observed in the burning rate behind behind the Mach shock originating from feature (5). In the simulation, the size of this region grows much faster compared to experiment, likely attributed to higher burning rates. It should be noted that the experiment [9] reports a velocity deficit up to 70% below the CJ velocity owing to losses from the channel walls. Since external losses are not accounted in the LES, and the CJ velocity is recovered, more rapid burning would be expected.

Finally, a grid resolution study was performed to ensure adequate convergence of the reaction rate of the LES. Figure 2 shows the averaged reactant mass fraction profiles of several LES and Euler simulations. To obtain the profiles shown, a quasi-1D representation is first obtained by Favre averaging across the channel height at any given time. The profiles are then ensemble-averaged for 50 random instances in time. Resolutions of the LES were varied from $h = (\lambda_{1/2}/8)$ to $h = (\lambda_{1/2}/64)$ while holding the number of subgrid nodes per LES cell, N, constant. For comparison, Euler simulations were also

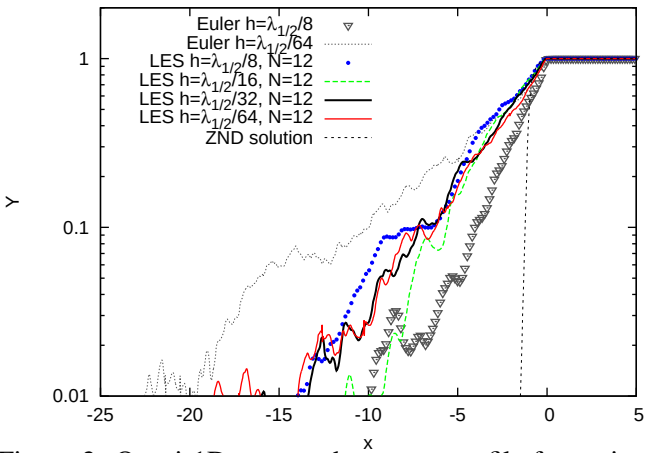

Figure 2: Quasi-1D averaged reactant profile for various LES and Euler simulation resolutions.

conducted at comparable resolutions. Clearly, as the resolution of the LES is increased beyond $h \geq (\lambda_{1/2}/32)$ with $N = 12$, the reactant mass fraction profiles collapse very well. Upon measuring the hydrodynamic thickness, Δ, taken as the distance from the shock, $x = 0$, to the location where $Y < 0.02$, the LES simulations converge to $\Delta = 13\lambda_{1/2}$. This is comparable to the experiment, which is estimated to be $\Delta \approx 9 - 12\lambda_{1/2}$. The Euler simulations, on the other hand, tend to increase in Δ with resolution. The Euler simulation with $h = (\lambda_{1/2}/64)$ was found to have $\Delta = 18\lambda_{1/2}$, much larger than LES and experiment [9].

5 Conclusions

In the current study, the CLEM-LES formulation has been extended to model 2-D detonation propagation. The results of the CLEM-LES have shown that qualitative features of a detonation triple point collision process are captured when compared to experiments [9]. Also, the CLEM-LES addresses a fundamental problem with Euler simulations; where reaction rates do not converge as resolution is increased. The LES was found to converge to, and capture, the correct approximate burning rates in the presence of Kelvin-Helmholtz and Richtmyer-Meshkov instabilities. The simulated hydrodynamic thickness is found to be comparable to experimental observation. In summary, the CLEM-LES is a fully conservative, high resolution, turbulent combustion model that reduces the complexities of a multi-dimensional problem to one-dimension and is able to handle highly compressible flows.

The Authors would like to acknowledge technical support from Andrej Pekalsi and Marc Leoine from Shell plc. Further support was provided by an NSERC Discovery Grant. Previous support has been provided by the Ontario Ministry of Training, Colleges and Universities via an Ontario Graduate Scholarship, a CFD Society of Canada Graduate Scholarship, and NSERC through an Alexander Graham Bell Scholarship, a Michael Smith Foreign Study Supplement, and the H2Can strategic network.

References

[1] M. I. Radulescu, G. J. Sharpe, C. K. Law, and J. H. S. Lee, "The hydrodynamic structure of unstable cellular detonations," *J. Fluid Mech.*, vol. 580, pp. 31–81, 2007.

[2] J. L. Ziegler, R. Deiterding, J. E. Shepherd, and D. I. Pullin, "An adaptive high-order hybrid scheme for compressive, viscous flows with detailed chemistry," *J. Comput. Phys.*, vol. 230, pp. 7598–7630, 2011.

[3] Y. Mahmoudi, N. Karimi, R. Deiterding, and S. Emami, "Hydrodynamic instabilities in gaseous detonations: comparison of euler, navierstokes, and large-eddy simulation," *Journal of Propulsion and Power*, vol. 30 No. 2, pp. 384–396, 2014.

[4] B. M. Maxwell, S. A. E. G. Falle, G. J. Sharpe, and M. I. Radulescu, *A compressible-LEM turbulent combustion model for assessing gaseous explosion hazards*. Bergen, Norway: Tenth International Symposium on Hazards, Prevention, and Mitigation of Industrial Explosions, 2014.

[5] S. Menon and A. R. Kerstein, *Turbulent Combustion Modeling: Advances, New Trends and Perspectives*. Springer, 2011, ch. 10: The Linear-Eddy Model, pp. 221–247.

[6] S. Menon and W. H. Calhoon, *Subgrid mixing and molecular transport modeling in a reacting shear layer*. Naples, Italy: 26th International Symposium on Combustion, 1996.

[7] V. K. Chakravarthy and S. Menon, "Subgrid modeling of turbulent premixed flames in the flamelet regime," *Flow, Turbulence and Combustion*, vol. 65, pp. 133–161, 2000.

[8] V. Sankaran and S. Menon, "LES of scalar mixing in supersonic mixing layers," *Proc. Combust. Inst.*, vol. 30, pp. 2835–2842, 2005.

[9] R. R. Bhattacharjee, "Experimental investigation of detonation re-initiation mechanisms following a mach reflection of a quenched detonation," Master's thesis, University of Ottawa, Ottawa, Canada, 2013.

[10] B. M. Maxwell and M. I. Radulescu, "Ignition limits of rapidly expanding diffusion layers: Application to unsteady hydrogen jets," *Combust. Flame*, vol. 158 No. 10, pp. 1946–1959, 2011.

[11] A. R. Kerstein, "Linear-eddy modeling of turbulent transport. part 6: Microstructure of diffusive scalar mixing fields," *Journal of Fluid Mechanics*, vol. 231, pp. 361–394, 1991.